Journal of Operation and Automation in Power Engineering
Vol. 7, No. 2, Oct. 2019, Pages: 176-186
http://joape.uma.ac.ir

# Maximum Power Point Tracker for Photovoltaic Systems Based on Moth-Flame Optimization Considering Partial Shading Conditions

*R. Aghaie* [1], *M. Farshad* [2,*]

[1]*Department of Electrical Engineering, Minoodasht Branch, Islamic Azad University, Minoodasht, Iran.*
[2]*Department of Electrical Engineering, Faculty of Basic Sciences and Engineering, Gonbad Kavous University, Gonbad Kavous, Iran.*

***Abstract-*** *The performance of photovoltaic (PV) systems is highly dependent on environmental conditions. Due to probable changes in environmental conditions, the real-time control of PV systems is essential for exploiting their maximum possible power. This paper proposes a new method to track the maximum power point of PV systems using the moth-flame optimization algorithm. In this method, the PV DC-DC converter's duty cycle is considered as the optimization parameter, and the delivered power of the PV system is maximized in real time. In the proposed approach, some schemes are also employed for detecting condition changes and ignoring small fluctuations of the duty cycle. The results of performance evaluation confirm that the proposed method is very fast, robust, and accurate in different conditions such as standard irradiance and temperature, irradiance and temperature variations, and partial shading conditions. The obtained steady-state efficiency and response time for the introduced method under the standard conditions of the test PV system are 99.68% and 0.021 s, respectively. Indeed, in addition to a relatively good efficiency, the faster response of the introduced tracker is also evident in comparison with other methods.*

***Keyword:*** maximum power point tracking, moth-flame optimization, partial shading condition, photovoltaic system.

## 1. INTRODUCTION

In recent years, the use of electrical energy generation systems based on renewable resources has increased due to environmental concerns, constrained fossil fuel resources, governmental incentives, and so on. One of the most common renewable electrical energy systems is the photovoltaic (PV) system. A challenge in these systems, like in many renewable energy systems, is preserving maximum efficiency during rapid changes in weather conditions.

To increase the efficiency of PV systems, researchers have focused on three main topics [1]: (a) designing solar irradiance tracking systems, (b) implementing efficient power converters, and (c) developing maximum power point tracking (MPPT) algorithms. The first two are mainly considered in designing and installing new PV systems, while MPPT algorithms have the potential to be employed in both new and existing PV systems [1].

Received: 22 Oct. 2018
Revised: 31 Dec. 2018
Accepted: 13 Feb. 2019
*Corresponding author:
E-mail: farshad@gonbad.ac.ir (M. Farshad)
Digital object identifier: 10.22098/joape.2019.5360.1401
***Research paper***


An MPPT algorithm should adjust the operating point of a PV system such that its output electrical power is maximized [2]. PV systems are connected to loads via DC-DC converters responsible for MPPT [3]. Indeed, the output of MPPT algorithms can be the reference current, reference voltage, or duty cycle of the pulse-width modulation (PWM) controller of DC-DC converters, and the operating point of PV systems can be controlled and adjusted via these parameters [4]. Under uniform irradiance, the power-voltage (P-V) curve of PV systems has only one maximum power point (MPP) which changes with temperature and irradiance variations. It is the task of MPPT algorithms to find new optimal operating points in line with these variations. Some conventional MPPT algorithms proposed for this purpose include perturbation and observation (P&O) [5], incremental conductance [5, 6], extremum-seeking control [7], and ripple correlation control [8].

Some elements of PV systems may receive lower irradiance due to the movement of clouds and shade of trees, buildings, and other adjacent objects; such a condition is called a partial shading condition (PSC). Under PSC which is very common and probable, there are several MPPs in the P-V curve of PV systems, one being the global maximum power point (GMPP), and the others called local maximum power point (LMPP) [9]. The location and amplitude of these points in P-V curves

depend on random changes in the shading pattern and arrangement of PV arrays. Researchers have found that, under PSC, the conventional MPPT methods which assume only one MPP on the P-V curve have a poor performance [10]. In fact, these methods cannot guarantee the convergence to GMPP, and they are often trapped in LMPPs due to their poor global search performance. For example, as a well-known conventional MPPT method, the P&O method has a low efficiency and may not converge to GMPP under PSC despite its fast convergence speed [11]. Owing to the shortcomings of the conventional MPPT algorithms, several methods have been proposed in recent years based on stochastic optimization and artificial intelligence algorithms [10], many of which have been reviewed in [12, 13]. The implementation of artificial intelligence-based MPPT algorithms using field-programmable gate arrays (FPGAs) has been discussed in [14]. In [15], an MPPT algorithm based on an improved form of the particle swarm optimization (PSO) algorithm in combination with the shuffled frog-leaping (SFL) algorithm has been presented, and its superior performance compared to the conventional MPPT methods has been demonstrated through comparative tests. Basic and modified versions of PSO have also been examined in MPPT strategies in [16-19]. Moreover, an MPPT approach based on a revised version of the genetic algorithm (GA) in combination with the conventional P&O method has been proposed in [20]. In [21], a modified form of the cat swarm optimization (CSO) algorithm has been utilized to track the GMPP of PV systems. Also, in [22], the cuckoo search optimization (CSO) algorithm has been employed to design an MPPT algorithm for PV systems. In [23], a modified version of the firefly algorithm (FA) has been used to improve the performance of the MPPT algorithm under PSC. An MPPT algorithm based on the flower pollination (FP) algorithm has also been proposed in [24]. Furthermore, an FP-based MPPT strategy has been introduced in [25] and compared to two other strategies based on differential evolution (DE) and PSO. In [26], the bat algorithm (BA) has been applied to enhance the tracking performance under PSC. Finally, an improved version of BA has been examined for developing an MPPT strategy in [11].

Although these reviewed soft-computing-based methods have shown appropriate performances in the PV MPPT studies, studies on newer and more powerful algorithms are still ongoing. Indeed, there are other ways to improve the efficiency and convergence speed of MPPT algorithms. This improvement can be achieved by employing more powerful global optimization algorithms which can more quickly and accurately reach the GMPP of PV systems under PSC.

In the present paper, the moth-flame optimization (MFO) algorithm is utilized to design a fast, robust, and accurate MPPT algorithm for PV systems. The MFO algorithm is a new and powerful method that has depicted its excellent performance in solving various optimization problems with numerous local optimum points [27]. The MFO algorithm has been employed as an enhancement of the incremental conductance MPPT algorithm for grid-connected PV plants through minimizing the error and optimizing the gain value [28]. However, to the best of the authors' knowledge, the MFO algorithm has not yet been applied and evaluated for the direct control of the duty cycle in the PV MPPT problem. In the introduced MPPT algorithm which directly controls the DC-DC converter's duty cycle, some schemes are also considered for the detection of condition changes and ignoring small fluctuations of the duty cycle. In fact, when the optimal operating point is found, another purpose is to prevent energy losses by operating PV modules without steady-state current and voltage fluctuations. In this paper, a PV system is simulated, and the performance of the proposed method is evaluated in various environmental conditions. In the next section, the MFO algorithm is introduced. In Section 3, the new MPPT algorithm is presented. In Section 4, the results of performance evaluation on the test PV system are provided. Finally, conclusions are drawn in Section 5.

## 2. MFO ALGORITHM

The MFO algorithm has been inspired by the spiral flying of moths around light sources, their navigation method, and their convergence towards light sources [27]. In this algorithm, the artificial moths are the candidate solutions of the optimization problem, and the optimization variables are their position coordinates in the search space. The artificial moths will fly in 1, 2, 3, or even higher dimensional spaces by varying their position vectors [27]. The MFO algorithm includes a population-based optimization procedure. In this algorithm, a set of artificial moths is considered in the following matrix form:

$$Mo = \begin{bmatrix} mo_{1,1} & mo_{1,2} \cdots mo_{1,d} \\ mo_{2,1} & mo_{2,2} \cdots mo_{2,d} \\ \vdots & \vdots \quad \cdots \vdots \\ mo_{n,1} & mo_{n,2} \cdots mo_{n,d} \end{bmatrix} \tag{1}$$

where $mo_{i,j}$ is the $j^{\text{th}}$ variable of the position vector of the

$i^{th}$ moth, $n$ is the number of artificial moths, and $d$ is the search space dimension.

To store the objective function or fitness values of the artificial moths, a vector is considered as:

$$FM = \begin{bmatrix} FM_1 \\ FM_2 \\ \vdots \\ FM_n \end{bmatrix} \tag{2}$$

where $FM_i$ is the objective function or fitness value of the $i^{th}$ moth.

Flames are another key component in the MFO algorithm. A matrix is also formed for flames as:

$$Fl = \begin{bmatrix} fl_{1,1} & fl_{1,2} \cdots fl_{1,d} \\ fl_{2,1} & fl_{2,2} \cdots fl_{2,d} \\ \vdots & \vdots \quad \cdots \vdots \\ fl_{n,1} & fl_{n,2} \cdots fl_{n,d} \end{bmatrix} \tag{3}$$

where $fl_{i,j}$ is the $j^{th}$ variable of the position vector of the $i^{th}$ flame. From the above relations, it can be inferred that the dimensions of matrices $Fl$ and $Mo$ are the same.

A vector is also considered for the flames to store the corresponding objective function or fitness values as:

$$FF = \begin{bmatrix} FF_1 \\ FF_2 \\ \vdots \\ FF_n \end{bmatrix} \tag{4}$$

where $FF_i$ is the objective function or fitness value of the $i^{th}$ flame.

It is worthy to note that both the moths and the flames are the candidate solutions of the optimization problem. The difference between them is due to the corresponding updating method. The moths are the main search agents flying in the search space, while the flames are the best position obtained by the moths so far. Indeed, the flames are similar to flags left by the moths while searching. Each artificial moth searches around an artificial flame and updates it if a better position is found. In this way, the best solution of moths will not be lost [27].

The MFO algorithm, which approximates the global optimum of optimization problems can be stated as:

$$MFO = (A, B, C) \tag{5}$$

where $A$ is a function generating an initial population and calculating their fitness values. The mathematical form of this function can be expressed as:

$$A \ : \ \phi \rightarrow \left\{ Mo, \ \ FM \right\} \tag{6}$$

Also, $B$ is the key function guiding the moths in the search space by updating matrix $Mo$:

$$B \ : \ Mo \rightarrow Mo \tag{7}$$

Function $C$ checks the stop criterion and returns *true* or *false* values:

$$C \ : \ Mo \rightarrow \{true, false\} \tag{8}$$

Using functions $A$, $B$, and $C$, the general structure of the MFO algorithm can be expressed as Ref. [27]:

$$\begin{aligned} &Mo = A(); \\ &while \ \ C(Mo) \ \ is \ \ equal \ \ to \ \ false \\ &\qquad Mo = B(Mo); \\ &end \end{aligned} \tag{9}$$

The MFO algorithm has been inspired by the moths' transverse orientation. To mathematically model this behavior, the position vectors of the moths are updated relative to the flames using the following equation:

$$Mo_i = SP(Mo_i, Fl_k) \tag{10}$$

where $Mo_i$ denotes the position vector of the $i^{th}$ moth, $Fl_k$ represents the position vector of the $k^{th}$ flame, and $SP$ indicates the spiral function. More details about the MFO algorithm are available in Ref. [27].

## 3. PROPOSED MPPT METHOD

In the proposed MPPT method, the duty cycle of the PV converter is optimized in real time by the MFO algorithm such that the PV power is maximized. The general schematic representation of the introduced method for a PV system with a buck DC-DC converter and the flowchart of the proposed MFO-based MPPT controller is depicted in Fig. 1. Based on Fig. 1(a), the output voltage and current of the PV module are continuously presented to the MFO-based MPPT controller, and this controller determines the duty cycle of the PWM generator in real time.

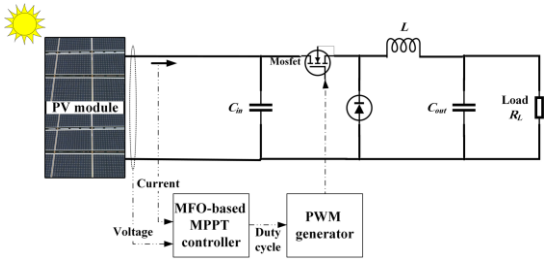


(a)

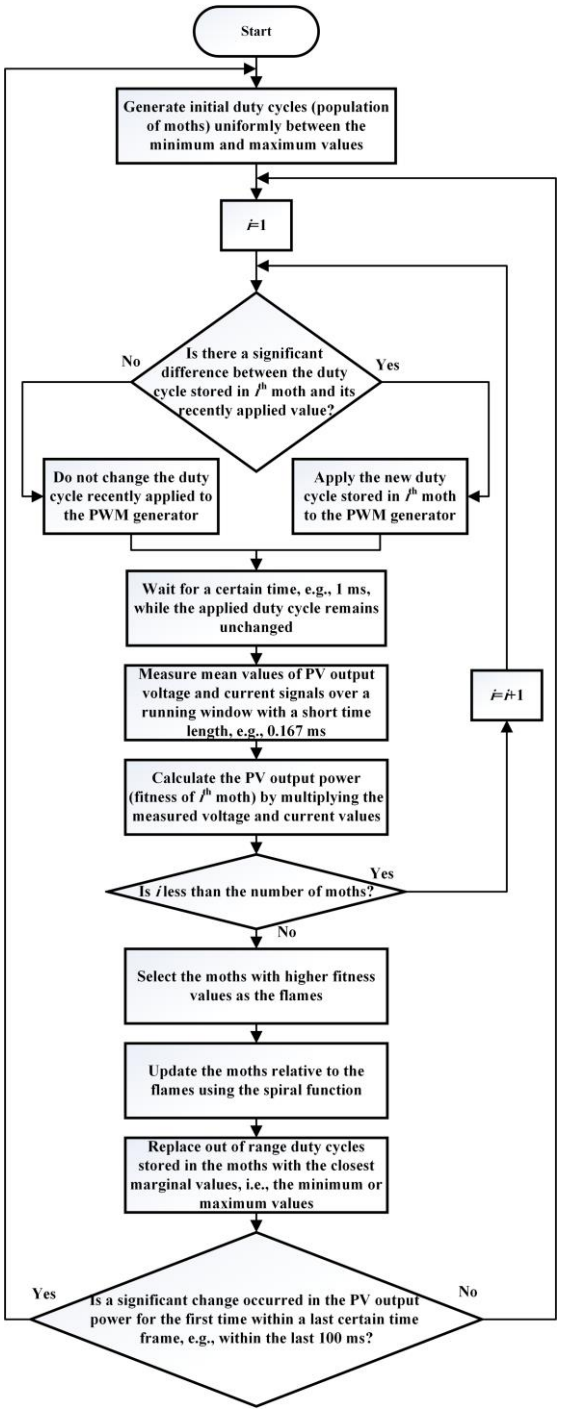


(b)

**Fig. 1. The proposed method: (a) General schematic view of a PV system with a buck converter, and (b) Flowchart of the MFO-based MPPT controller**

In the method used in this paper, the optimization problem solved by the MFO algorithm is as follows:

$$\max_{D}(V_{pv} \times I_{pv}) = \max_{D}(P_{pv})$$

$$\text{s.t.} \quad (11)$$

$$D_{\min} \le D \le D_{\max}$$

where $V_{pv}$, $I_{pv}$, and $P_{pv}$ are the output voltage, current, and power of the PV module, respectively. Moreover, $D$ indicates the DC-DC converter's duty cycle, and $D_{min}$ and $D_{max}$ stand for the minimum and maximum duty cycles, respectively.

In the proposed method, the following spiral function is used for updating in the MFO algorithm:

$$SP(Mo_i, Fl_k) = r_1.\left|Fl_k - Mo_i\right|.e^{(g-t)} + r_2.Fl_k \quad (12)$$

where $r_1$ is a random number in [0, 1]; $r_2$ is a random number close to 1, for example, in [0.995, 1]; $g$ is a random number in [-1, 1]; and $t$ is the damping coefficient. The value of $t$ is 1 in the first iteration, and in the next iterations, an inverse number of moths is added to it. As the number of iterations increases, $t$ decreases the effect of the first part of the updating function.

Based on Fig. 1(b), the MFO algorithm requires an initial population of solutions to start. In this paper, these initial solutions are generated with a uniform distribution and distance between minimum and maximum duty cycles.

It is clear that the MFO algorithm in the introduced method should be executed continuously as a function. To implement the MFO algorithm in the proposed MPPT method, some points should be considered:

a) A short time interval, for example, 0.001 s, is considered between consecutive fitness calculations in the MFO algorithm to have sufficient time for receiving the impact of the MPPT controller output on the output of the PV system. At times between two consecutive fitness calculations in the MFO algorithm, the controller's output remains unchanged.

b) A scheme is assumed for detecting changes in the output of the PV system so that the MFO algorithm is reset and begins to optimize the duty cycle with the initial population only when a significant change occurs. This scheme operates on the basis of the absolute derivative of the PV output power. After resetting the MFO algorithm, this scheme is automatically disabled for a certain time which should be larger than the convergence time of the MFO algorithm, for instance, 0.1 s, to have enough time for convergence and finding the new optimal operating point.

c) A scheme is considered for ignoring small fluctuations of the duty cycle, for instance, less than 1%, so that the PV modules are operated without steady-state current and voltage fluctuations after the convergence of the MFO algorithm. This scheme will prevent energy losses.

Fig. 2 depicts a more detailed schematic representation of the proposed MPPT controller prepared in Simulink/MATLAB. The implemented schemes for detecting changes and resetting the MFO algorithm and ignoring small fluctuations of the duty cycle are specified in this figure.

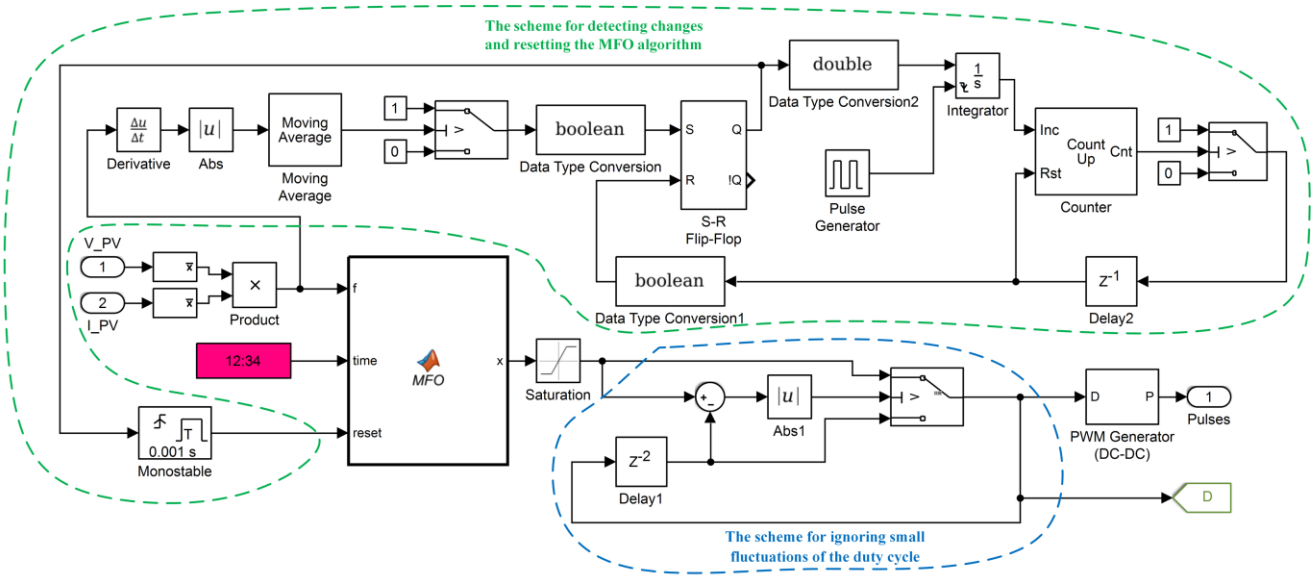


**Fig. 2. The proposed MPPT controller prepared in Simulink/MATLAB**

## 4. RESULTS AND DISCUSSION

To evaluate the introduced method, the PV system of Fig. 1(a) is simulated in Simulink/MATLAB. The characteristics of the converter and PV module in the standard conditions are provided in Tables 1 and 2, respectively. The single-diode five-parameter PV model is employed in the simulations. The minimum and maximum duty cycles of the converter are set to 0.3 and 0.6, respectively, Also, the population size of artificial moths in the MFO algorithm is determined as 8.

**Table 1. Characteristics of buck DC-DC converter elements [4]**

| Parameter | Value |
|---|---|
| Load resistance ($R_L$) | 1 (Ω) |
| Inductance ($L$) | 300 (μH) |
| Input capacitance ($C_{in}$) | 100 (μF) |
| Output capacitance ($C_{out}$) | 990 (μF) |
| Switching frequency of the PWM generator | 100 kHz |

**Table 2. Characteristics of PV module in the standard conditions [4, 29]**

| Parameter | Value |
|---|---|
| Model | KC200GT |
| Maximum power | 200.143 (W) |
| Voltage at MPP | 26.3 (V) |
| Current at MPP | 7.61 (A) |
| Open-circuit voltage | 32.9 (V) |
| Short-circuit current | 8.21 (A) |
| Temperature coefficient of open-circuit voltage | -0.35502 (%/ºC) |
| Temperature coefficient of short-circuit current | 0.06 (%/ºC) |
| Cells per module | 54 |

### 4.1. Performance under standard conditions

Here, the performance of the proposed method is evaluated through simulation of the test PV system under standard conditions, signifying the temperature of 25 ºC and the solar irradiance of 1000 W/m$^2$. Fig. 3 illustrates the proposed MPPT controller's output duty cycle, PV output voltage, load voltage, PV output current, load current, and PV output power.

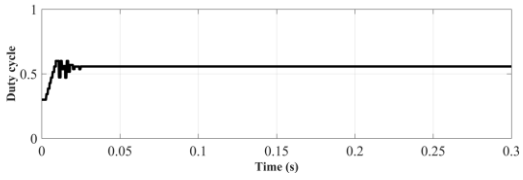


(a)

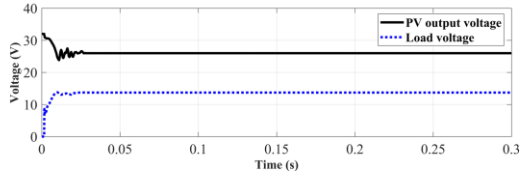


(b)

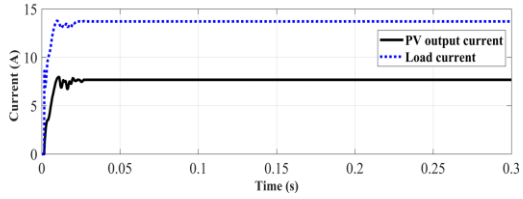


(c)

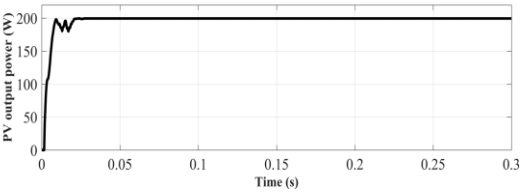


(d)

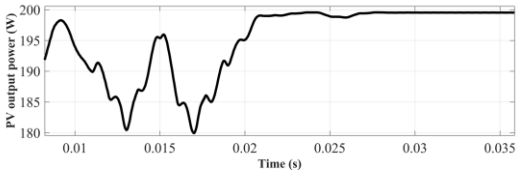


(e)

**Fig. 3. Test under standard conditions: (a) Duty cycle, (b) Voltage, (c) Current, (d) PV power, and (e) PV power (with magnification)**

Comparing the data provided in Table 2 for the standard conditions and Figs. 3(b)-3(d), it can be comprehended that the PV output voltage, current, and power have tended to their nominal values. By investigating Fig. 3(e), it can be observed that the response speed of the proposed MPPT algorithm under standard conditions is very high, and the algorithm has converged to the optimum solution in about 0.021 s after being started. Furthermore, the steady-state output power is about 199.5 W which is very close to the PV maximum power, i.e., 200.143 W.

### 4.2. Performance under irradiance variations

Here, the introduced method is evaluated under the standard temperature of 25 ºC and variable irradiation. Initial irradiance when the system starts operation is 400 W/m$^2$ which reaches 600, 800, and 1000 W/m$^2$ in 0.2, 0.4, and 0.6 s, respectively. The output duty cycle of the proposed MPPT controller, PV output voltage, load voltage, PV output current, load current, and PV output power for this test are provided in Fig. 4. Based on Fig. 4, the irradiance variations have been well detected, and the algorithm has converged to the new optimum solutions with good speed. The P-V curves of the test PV module under the standard temperature and the irradiances of 400, 600, 800, and 1000 W/m$^2$ are given in Fig. 5. Comparing Fig. 4(d) and Fig. 5, it can be inferred that the proposed algorithm has converged to the true MPPs under various irradiances.

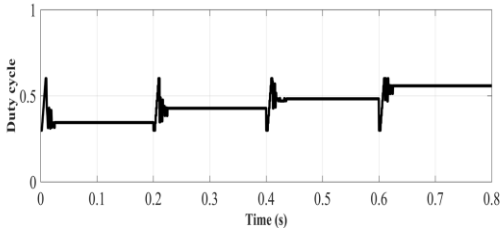


(a)

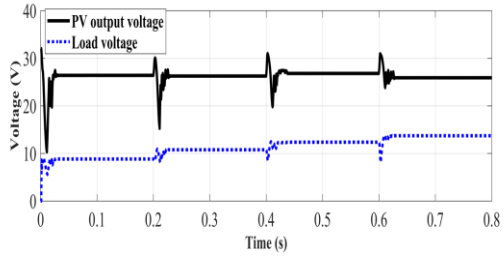


(b)

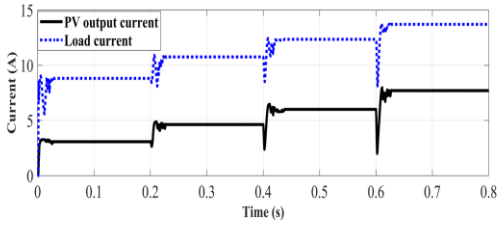


(c)

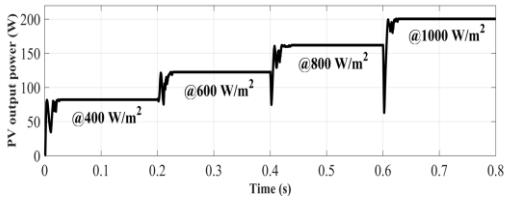


(d)

**Fig. 4. Test under variable irradiation: (a) Duty cycle, (b) Voltage, (c) Current, and (d) PV power**

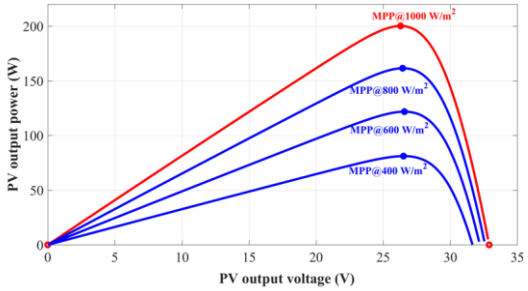


**Fig. 5. P-V curves for the test PV module under various irradiances**

### 4.3. Performance under temperature variations

In this test, the performance of the proposed method is evaluated under the standard irradiance of 1000 W/m$^2$ and variable temperature. The initial temperature when the PV system is started is 45 ºC which decreases to 25 and 5 ºC in 0.25 and 0.5 s, respectively. Fig. 6 depicts the controller's output duty cycle, PV output voltage, load voltage, PV output current, load current, and PV output power for this test.

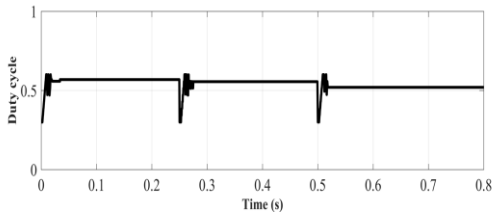


(a)

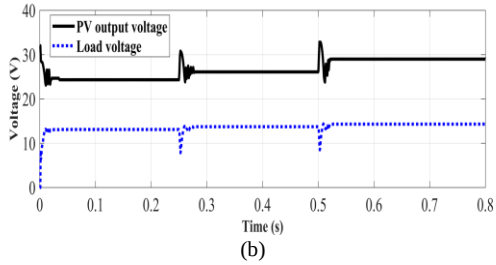


(b)

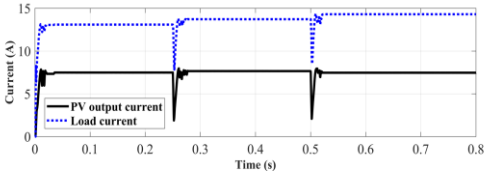


(c)

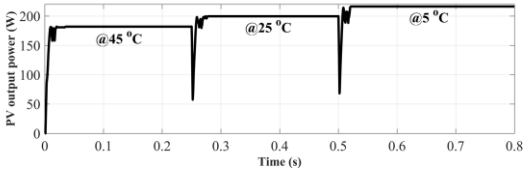


(d)

Fig. 6. Test under variable temperature: (a) Duty cycle, (b) Voltage, (c) Current, and (d) PV power

Investigating Fig. 6, it can be concluded that the temperature variations have been well detected, and the algorithm has a good convergence speed. The P-V curves of the test PV module under the standard irradiance and the temperatures of 45, 25, and 5 ºC are given in Fig. 7. Comparing Fig. 6(d) and Fig. 7, it can be understood that the introduced algorithm has efficiently tracked the true MPPs under different temperatures.

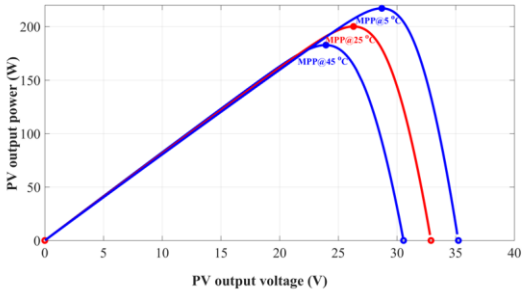


Fig. 7. P-V curve for the test PV module under various temperatures

### 4.4. Performance under PSC

Here, an array comprising three series PV modules with the characteristics given in Table 2 is simulated in Simulink/MATLAB as demonstrated in Fig. 8.

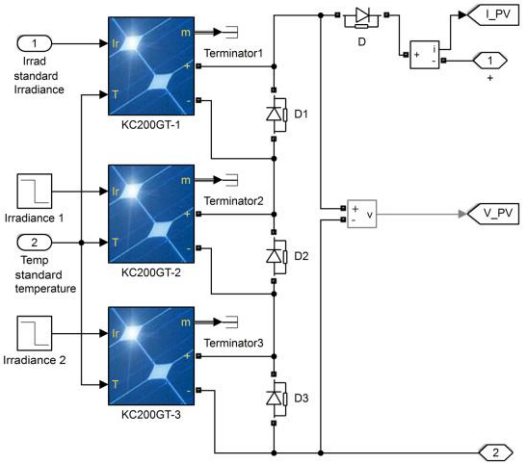


**Fig. 8. The test array comprising three PV modules for simulating PSC in Simulink/MATLAB**

Before PSC, all three modules of the simulated array are utilized under the standard temperature of 25 ºC and the standard irradiance of 1000 W/m$^2$. At 0.4 s, the irradiances of the second and third modules are decreased to 650 and 350 W/m$^2$, respectively, while the irradiance of the first module remains as before. The output duty cycle of the proposed controller, PV output voltage, load voltage, PV output current, load current, and PV output power for this test condition are shown in Fig. 9.

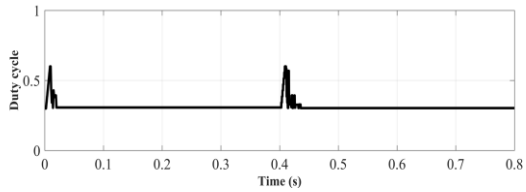


(a)

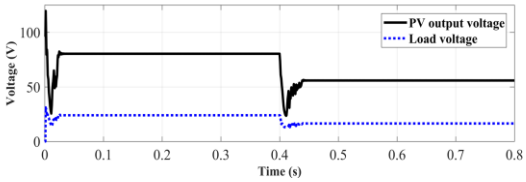


(b)

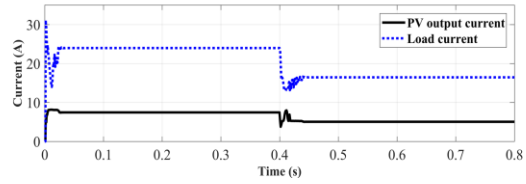


(c)

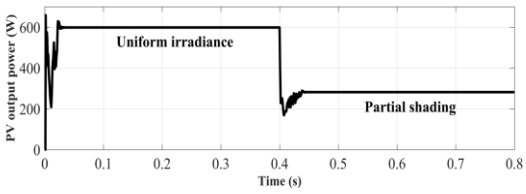


(d)

**Fig. 9. Test under PSC: (a) Duty cycle, (b) Voltage, (c) Current, and (d) PV power**

As evident from Fig. 9, the proposed MPPT algorithm has correctly detected the PSC and converged with a proper speed. Nevertheless, in the PSC, the convergence time has increased by about 0.02 s compared to the standard conditions in which the P-V curve had only one MPP. The current-voltage (I-V) and P-V curves of the test PV array under the uniform irradiance and the PSC are presented in Fig. 10. By comparing Figs. 9 and 10, it can be deduced that the proposed controller has successfully tracked the true MPP under the uniform irradiance. Furthermore, this algorithm has found the true GMPP under the PSC, and it has not been trapped in the two LMPPs specified in Fig. 10(b).

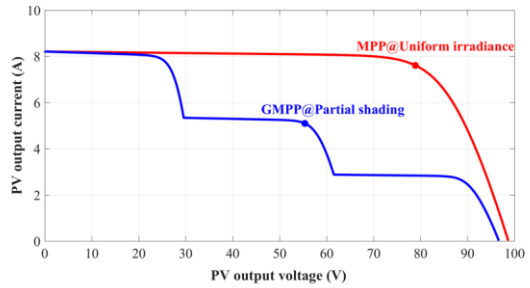


(a)

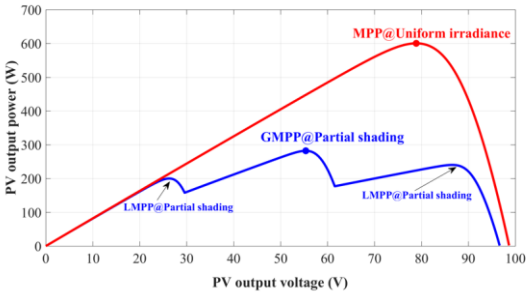


(b)

**Fig. 10. Curves for the test PV array under uniform irradiance and PSC: (a) I-V, and (b) P-V**

### 4.5. Comparison with other methods

In this section, the performance of the proposed MPPT algorithm is compared to that of other methods. Characteristics of the simulated PV system are adopted from the sample system of [4]. In this reference, in addition to a new MPPT method based on the golden section optimization (GSO) algorithm, three other MPPT methods, including P&O, hill-climbing fuzzy logic [30], and adaptive P&O fuzzy logic [31] have also been tested on the sample system. The GSO-based MPPT algorithm introduced in [4] does not directly control the converter's duty cycle. Thus, here, the GSO algorithm is reprogrammed to directly control the converter's duty cycle as well, and the results of all methods are compared with those of the proposed MFO-based MPPT method, as given in Table 3. It should be noted that the test results provided in this table relate to the standard conditions. Also, in this table, the method's efficiency is considered as the ratio of the steady-state power to the maximum power. Based on Table 2, the PV maximum power under standard conditions is 200.143 W. The steady-state efficiency values provided in the third column of Table 3 have been calculated by dividing the steady-state output power values presented in the second column by 200.143 W. According to Table 3, the efficiency of the introduced controller is slightly less than the efficiencies of two methods, including the adaptive P&O fuzzy logic method in Ref. [31] and the GSO-based method with direct control of the duty cycle.

**Table 3. Comparing the proposed method to other methods**

| MPPT Method | Response time (s) | Steady-state output power (W) | Steady-state efficiency (%) | Steady-state error (W) |
|---|---|---|---|---|
| The proposed MFO-based method | 0.021 | 199.5 | 99.68 | 0.643 |
| The reprogrammed GSO-based method with direct control of the duty cycle | 0.042 | 199.7 | 99.78 | 0.443 |
| The GSO-based method [4] | 0.025 | 199 | 99.43 | 1.143 |
| The P&O method [4] | 0.069 | 197.8 | 98.83 | 2.343 |
| The hill-climbing fuzzy logic method [4, 30] | 0.055 | 199.5 | 99.68 | 0.643 |
| The adaptive P&O fuzzy logic method [4, 31] | 0.04 | 200.1 | 99.98 | 0.043 |

However, the response time of the proposed method is about half the response time of these methods. Indeed, from among the methods compared in Table 3, the proposed MFO-based method has the fastest response. For more comparison under standard conditions and the PSC, performances of the MFO-based method and the GSO-based method with direct control of the duty cycle are presented in Fig. 11. According to this figure, under both the standard conditions and the PSC, the convergence speed of the proposed MFO-based method is higher.

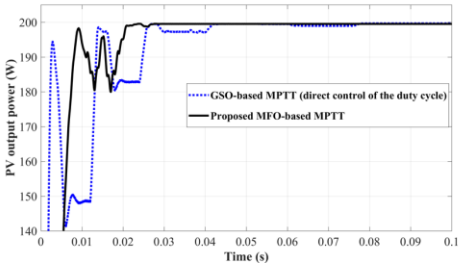


(a)

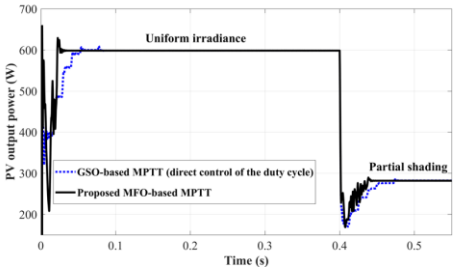


(b)

**Fig. 11. Performances of the MFO-based method and the GSO-based method with direct control of the duty cycle: (a) under standard conditions, and (b) under PSC**

### 4.6. Performance in a system with boost converter

The introduced method can be applied with the boost converter as well. Here, a system similar to the test system of Ref. [11] is also simulated, and the proposed method is compared to other methods in an equally fair condition using this system. The general schematic view of the simulated PV system with the boost converter is

illustrated in Fig. 12. Moreover, the characteristics of the boost converter are presented in Table 4. The minimum and maximum duty cycles of the converter are set to 0.4 and 0.7, respectively. The P-V curve of the test PV array [11] under the standard conditions is also shown in Fig. 13. Based on this figure, the PV maximum power is 366.06 W.

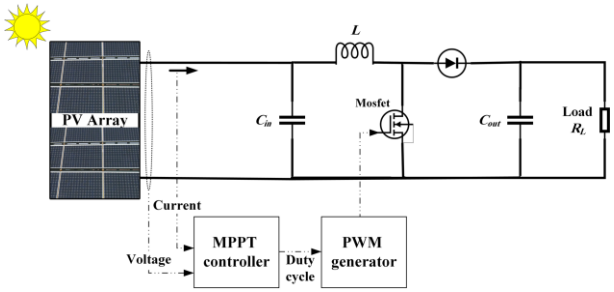


**Fig. 12. General schematic view for the PV system with a boost converter**

**Table 4. Characteristics of boost DC-DC converter elements [11]**

| Parameter | Value |
|---|---|
| Load resistance ($R_L$) | 150 (Ω) |
| Inductance ($L$) | 12 (mH) |
| Input capacitance ($C_{in}$) | 50 (μF) |
| Output capacitance ($C_{out}$) | 100 (μF) |
| Switching frequency of the PWM generator | 10 kHz |

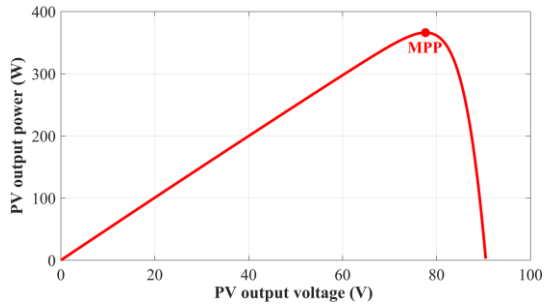


**Fig. 13. P-V curve for the test PV array under standard conditions**

Fig. 14 illustrates the controller's output duty cycle, PV output voltage, load voltage, PV output current, load current, and PV output power for the new test system employing both the proposed method and the reprogrammed GSO-based method with direct control of the duty cycle.

It is clear from Fig. 14 that both methods have correctly tracked the MPP; nevertheless, the convergence speed of the proposed method seems to be superior compared to the GSO-based method. In [11], some MPPT methods have been evaluated and compared in a test system similar to the one simulated here. In Table 5, the results for the GSO- and MFO-based MPPT methods are provided in addition to the comparison of the results of [11].

Based on Table 5, the efficiency of the introduced MFO-based method is greater than the efficiencies of all the methods compared, except for the GSO-based method. However, the proposed method has a higher convergence speed compared to the GSO-based method.

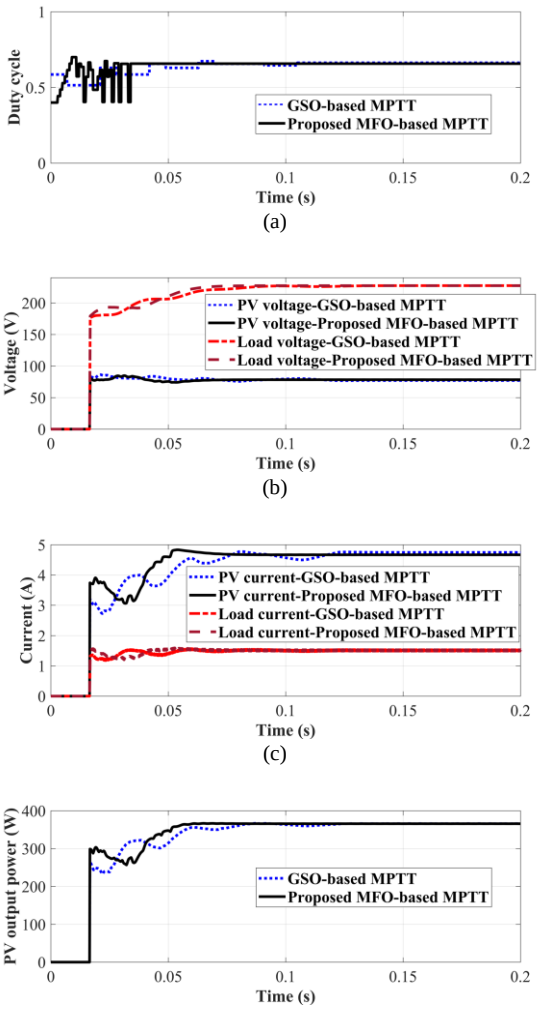


**Fig. 14. Performances of the MFO-based method and the GSO-based method with direct control of the duty cycle: (a) Duty cycle, (b) Voltage, (c) Current, and (d) PV power**

**Table 5. Comparing the proposed method with other methods in the test system with the boost converter**

| MPPT Method | Response time (s) | Steady-state output power (W) | Steady-state efficiency (%) | Steady-state error (W) |
|---|---|---|---|---|
| The proposed MFO-based method | 0.040 | 365.70 | 99.90 | 0.36 |
| The reprogrammed GSO-based method with direct control of the duty cycle | 0.069 | 365.90 | 99.96 | 0.16 |
| P&O method [11] | 0.002 | 320.90 | 87.66 | 45.16 |
| Improved P&O method [11] | 0.011 | 323.18 | 88.29 | 42.88 |
| PSO-based method [11] | 0.003 | 365.33 | 99.80 | 0.73 |
| BA-based method [11] | 0.017 | 365.03 | 99.72 | 1.03 |
| FA-based method [11] | 0.110 | 332.05 | 90.71 | 34.01 |
| FP-based method [11] | 0.022 | 365.36 | 99.81 | 0.70 |
| Artificial bee colony-based method [11] | 0.068 | 364.95 | 99.70 | 1.11 |
| Improved BA-based method [11] | 0.015 | 365.59 | 99.87 | 0.47 |

### 4.7. Considerations in converter design

In practice, the inductance and capacitance values of the converter have considerable effects on the output peak-to-peak voltage ripple. Maintaining the output voltage ripple in an acceptable range is usually a converter design problem [32, 33].

Furthermore, the current ripple has important effects on the loss, efficiency, and lifespan of power electronic systems [34, 35]. Minimization of the input current ripple is critical for PV systems since it has a direct effect on the MPPT controller's performance. Indeed, the MPP can be tracked accurately if the input current ripple is zero or very low [34]. This is usually a converter design problem, too.

The switching frequency is another influential parameter. Although a high switching frequency will result in a smaller and cheaper converter and will improve the transient response, it will also increase the switching loss. This paper contains the test results for two different test systems adapted from recently published papers [4, 11]. The results indicate that the proposed MPPT controller can perform well under both converter designs.

## 5. CONCLUSIONS

A new MFO-based method has been presented for tracking the maximum power point of PV systems. In this method, the DC-DC converter's duty cycle is optimized directly by the MFO algorithm through which the PV output power is maximized. In this method, two schemes have also been designed for the detection of sudden condition changes and elimination of small fluctuations of the duty cycle. The performance of the proposed method has been verified on a PV system under different conditions. According to the test results, the proposed MPPT controller has a fast, robust, and accurate performance under standard conditions. Furthermore, the proposed method can detect irradiance and temperature variations and track the true MPPs. The performance of the introduced method under PSC is acceptable and accurate as well, and this method converges to GMPP without being trapped in local optimums.

## REFERENCES


[1] H. Yatimi and E. Aroudam, "Assessment and control of a photovoltaic energy storage system based on the robust sliding mode MPPT controller," *Solar Energy*, vol. 139, pp. 557-568, December 2016.

[2] J. Javidan, "Energy management strategy of stand-alone photovoltaic system in cathodic protection pipeline," *J. Oper. Autom. Power Eng.*, vol. 4, no. 2, pp. 143-152, 2016.

[3] A. Hatefi Einaddin, A. Sadeghi Yazdankhah, and R. Kazemzadeh, "Power management in a utility connected micro-grid with multiple renewable energy sources," *J. Oper. Autom. Power Eng.*, vol. 5, no. 1, pp. 1-10, 2017.

[4] A. Kheldoun, R. Bradai, R. Boukenoui, and A. Mellit, "A new Golden Section method-based maximum power point tracking algorithm for photovoltaic systems," *Energy Convers. Manage.*, vol. 111, pp. 125-136, March 2016.

[5] V. Jately and S. Arora, "Development of a dual-tracking technique for extracting maximum power from PV systems under rapidly changing environmental conditions," *Energy*, vol. 133, pp. 557-571, August 2017.

[6] J. Ghazanfari and M. Maghfoori Farsangi, "Maximum power point tracking using sliding mode control for photovoltaic array," *Iran. J. Electr. Electron. Eng.*, vol. 9, no. 3, pp. 189-196, 2013.

[7] P. Lei, Y. Li, and J. E. Seem, "Sequential ESC-Based Global MPPT Control for Photovoltaic Array With Variable Shading," *IEEE Trans. Sustain. Energy*, vol. 2, no. 3, pp. 348-358, July 2011.

[8] P. Midya, P. T. Krein, R. J. Turnbull, R. Reppa, and J. Kimball, "Dynamic maximum power point tracker for photovoltaic applications," *PESC Record. 27th Annu. IEEE Power Electron. Specialists Conf.*, 1996, pp. 1710-1716 vol.2.

[9] K. Sundareswaran, V. Vignesh kumar, and S. Palani, "Application of a combined particle swarm optimization and perturb and observe method for MPPT in PV systems under partial shading conditions," *Renewable Energy*, vol. 75, pp. 308-317, March 2015.

[10] N. A. Kamarzaman and C. W. Tan, "A comprehensive review of maximum power point tracking algorithms for photovoltaic systems," *Renewable Sustain. Energy Rev.*, vol. 37, pp. 585-598, September 2014.

[11] Z. Wu and D. Yu, "Application of improved bat algorithm for solar PV maximum power point tracking under partially shaded condition," *Appl. Soft Comput.*, vol. 62, pp. 101-109, January 2018.

[12] L. L. Jiang, R. Srivatsan, and D. L. Maskell, "Computational intelligence techniques for maximum power point tracking in PV systems: A review," *Renewable Sustain. Energy Rev.*, vol. 85, pp. 14-45, April 2018.

[13] A. Mellit and S. A. Kalogirou, "MPPT-based artificial intelligence techniques for photovoltaic systems and its implementation into field programmable gate array chips: Review of current status and future perspectives," *Energy*, vol. 70, pp. 1-21, June 2014.

[14] F. Chekired, A. Mellit, S. A. Kalogirou, and C. Larbes, "Intelligent maximum power point trackers for photovoltaic applications using FPGA chip: A comparative study," *Solar Energy*, vol. 101, pp. 83-99, March 2014.

[15] M. Mao, L. Zhang, P. Duan, Q. Duan, and M. Yang, "Grid-connected modular PV-Converter system with shuffled frog leaping algorithm based DMPPT controller," *Energy*, vol. 143, pp. 181-190, January 2018.

[16] M. Mao, L. Zhang, Q. Duan, and B. Chong, "Multilevel DC-link converter photovoltaic system with modified PSO based on maximum power point tracking," *Solar Energy*, vol. 153, pp. 329-342, September 2017.

[17] G. Dileep and S. N. Singh, "An improved particle swarm optimization based maximum power point tracking algorithm for PV system operating under partial shading conditions," *Solar Energy*, vol. 158, pp. 1006-1015, December 2017.

[18] H. Chaieb and A. Sakly, "A novel MPPT method for photovoltaic application under partial shaded conditions," *Solar Energy*, vol. 159, pp. 291-299, January 2018.

[19] M. Sarvi, S. Ahmadi, and S. Abdi, "A PSO-based maximum power point tracking for photovoltaic systems under environmental and partially shaded conditions," *Prog. Photovoltaics: Res. Appl.*, vol. 23, no. 2, pp. 201-214, 2015.

[20] S. Daraban, D. Petreus, and C. Morel, "A novel MPPT (maximum power point tracking) algorithm based on a modified genetic algorithm specialized on tracking the global maximum power point in photovoltaic systems affected by partial shading," *Energy*, vol. 74, pp. 374-388, September 2014.

[21] L. Guo, Z. Meng, Y. Sun, and L. Wang, "A modified cat swarm optimization based maximum power point tracking method for photovoltaic system under partially shaded condition," *Energy*, vol. 144, pp. 501-514, February 2018.

[22] J. Ahmed and Z. Salam, "A Maximum Power Point Tracking (MPPT) for PV system using Cuckoo Search with partial shading capability," *Appl. Energy*, vol. 119, pp. 118-130, April 2014.

[23] D. F. Teshome, C. H. Lee, Y. W. Lin, and K. L. Lian, "A Modified Firefly Algorithm for Photovoltaic Maximum Power Point Tracking Control Under Partial Shading," *IEEE J. Emerging Sel. Top. Power Electron.*, vol. 5, no. 2, pp. 661-671, June 2017.

[24] J. Prasanth Ram and N. Rajasekar, "A new global maximum power point tracking technique for solar photovoltaic (PV) system under partial shading conditions (PSC)," *Energy*, vol. 118, pp. 512-525, January 2017.

[25] A. A. Zaki Diab and H. Rezk, "Global MPPT based on flower pollination and differential evolution algorithms to mitigate partial shading in building integrated PV system," *Solar Energy*, vol. 157, pp. 171-186, November 2017.

[26] K. Kaced, C. Larbes, N. Ramzan, M. Bounabi, and Z. e. Dahmane, "Bat algorithm based maximum power point tracking for photovoltaic system under partial shading conditions," *Solar Energy*, vol. 158, pp. 490-503, December 2017.

[27] S. Mirjalili, "Moth-flame optimization algorithm: A novel nature-inspired heuristic paradigm," *Knowl.-Based Syst.*, vol. 89, pp. 228-249, November 2015.

[28] N. Aouchiche, M. S. Aitcheikh, M. Becherif, and M. A. Ebrahim, "AI-based global MPPT for partial shaded grid connected PV plant via MFO approach," *Solar Energy*, vol. 171, pp. 593-603, 2018/09/01/ 2018.

[29] "*MATLAB User's Guide: R2017a Documentation,*" MathWorks Inc, Natick, MA, USA, 2017.

[30] B. N. Alajmi, K. H. Ahmed, S. J. Finney, and B. W. Williams, "Fuzzy-Logic-Control Approach of a Modified Hill-Climbing Method for Maximum Power Point in Microgrid Standalone Photovoltaic System," *IEEE Trans. Power Electron.*, vol. 26, no. 4, pp. 1022-1030, April 2011.

[31] M. A. A. M. Zainuri, M. A. M. Radzi, A. C. Soh, and N. A. Rahim, "Development of adaptive perturb and observe-fuzzy control maximum power point tracking for photovoltaic boost dc-dc converter," *IET Renewable Power Gener.*, vol. 8, no. 2, pp. 183-194, March 2014.

[32] E. Babaei and M. E. S. Mahmoodieh, "Calculation of output voltage ripple and design considerations of SEPIC converter," *IEEE Trans. Ind. Electron.*, vol. 61, no. 3, pp. 1213-1222, March 2014.

[33] S. Liu, Y. Li, and L. Liu, "Analysis of output voltage ripple of buck DC-DC converter and its design," in *2009 2nd Int. Conf. Power Electron. Intell. Transport. Sys. (PEITS)*, 2009, pp. 112-115.

[34] A. H. E. Khateb, N. A. Rahim, J. Selvaraj, and B. W. Williams, "DC-to-DC converter with low input current ripple for maximum photovoltaic power extraction," *IEEE Trans. Ind. Electron.*, vol. 62, no. 4, pp. 2246-2256, April 2015.

[35] E. Salary, M. R. Banaei, and A. Ajami, "Multi-stage DC-AC converter based on new DC-DC converter for energy conversion," *J. Oper. Autom. Power Eng.*, vol. 4, no. 1, pp. 42-53, 2016.